PHYS. MED. BIOL., 1976, VOL. 21, NO. 4, 560–569. © 1976

Quantitative Proton Tomography: Preliminary Experiments

A. M. CORMACK M.SC.

Physics Department, Tufts University, Medford, MA 02155, U.S.A.

A. M. KOEHLER B.A.

Cyclotron Laboratory, Harvard University, Cambridge, MA 02138, U.S.A.

Received 14 *October* 1975

ABSTRACT. An attempt has been made to see whether energetic protons (158 MeV) could be used instead of X-rays in computerized axial tomography to detect density differences of the order of those at which commercial X-ray tomographs cease to be useful. A circularly symmetrical phantom consisting of Lucite and sugar solutions was used, and density differences of 0·5% were reconstructed with reasonable accuracy from data obtained with very simple equipment. Discontinuities in either density or chemical composition, or both, seem to cause artifacts in the reconstruction. These may be related to the West–Sherwood effect.

1. Introduction

The quantitative use of the absorption of X-rays in a technique known in medical circles as Computerized Axial Tomography (CAT) has increased enormously since commercial devices for the implementation of the technique came on the market a few years ago. These devices produce X-ray tomographs which can reliably detect density differences in soft tissue of 1% over regions of a few square millimetres, and could presumably detect even smaller density differences at the cost of a considerable increase in the radiation dose received by the object being examined.

In the first papers on this technique (Cormack 1963, 1964) it was pointed out that the essential part of the technique, the reconstruction problem, had other possible applications such as positron annihilation radiation scanning, and tomography using heavy charged particles, for example protons. The latter suggestion, which is the subject of this paper, was not then made with much force because of doubts which were subsequently laid to rest by Koehler (1968). He showed that, by using parallel-sided objects with a thickness nearly equal to the range of the incident proton beam, one could record on film radiographs showing much greater contrast than X-radiographs taken under the same conditions. Extension of this technique to the examinations of human material has been explored by Stewart and Koehler (1973, 1974). The sharpness of the images in these proton radiographs suggests that the multiple scattering of protons by the specimen may not be too much of an impediment to obtaining useful proton tomographs. Indeed, a successful tomograph has been demonstrated by Crowe, Budinger, Cahoon, Elischer, Huesman and Kanstein (1975) using 910 MeV helium ions, but analysis of their results in terms of the ultimate limits of the technique is difficult. The problem then is not whether the reconstruction process will produce a proton tomograph, but rather how good the tomograph will be, and what advantages and disadvantages a proton tomograph will have over an X-ray tomograph because of the difference between the interactions of protons and X-rays with matter.

The experiment described below has been a first step in investigating the problems of proton tomography using a simple phantom with density differences between its components of 1% or less, roughly the level at which commercial X-ray tomographs cease to be useful. The apparatus used was rudimentary, and its dynamic range was small but sufficient for our purposes. This small dynamic range is not inherent in proton tomography, and it is easy to imagine quite different detector systems with large dynamic range.

2. Experimental arrangement

The arrangement of the equipment is shown in fig. 1. The 158 MeV external beam of the Harvard cyclotron is focused, through a 6 mm hole in collimator A, on a lead foil 3·51 g cm^{-2} thick which scatters the beam so that collimators B, C and D define two small beams at an angle of 1·33° above and below the horizontal. All collimators were made of brass 3·8 cm thick. These beams are

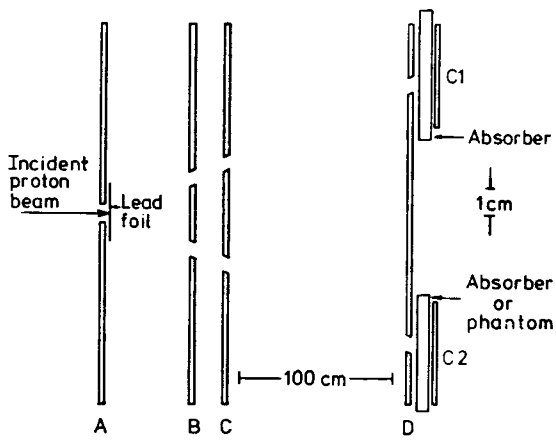

Fig. 1. Incident protons are scattered by the lead foil. Two beams in a vertical plane are defined by holes in collimators B, C and D. The protons are detected by scintillation counters C1 and C2.

detected by two sodium iodide scintillation counters C1 and C2. The rest of the scattered proton beam is stopped by the collimators and this results in a beam-associated background of neutrons and γ-rays in the experimental area. The scintillators were 3·81 cm in diameter and 2·54 cm thick, and they were mounted on R.C.A. 6810A photomultipliers. The currents from the photomultipliers were fed to two current integrators arranged so that when a predetermined charge had been accumulated from one (the monitor counter) the cyclotron would be turned off and the amount of charge from the other detector measured.

The vertical plane for the proton beams was chosen to minimize the effects of variation in the position of the primary external beam. These variations occur because of small variations in the currents of the main cyclotron magnet and the bending and focusing magnets along the external beam, and are expected to be less in the vertical plane than the horizontal. We believe that vertical fluctuations in the position of the primary beam are the main source of the fluctuations in our data. A beam configuration less sensitive to shifts in the incident beam but requiring more detectors than we have at present will be used in further experiments.

3. Experimental procedure

Using one counter as a preset monitor, the voltage on the integrating capacitor of the other counter was measured as a function of the amount of plastic absorber (Lucite) placed after collimator D in the 'active' beam. Fig. 2 shows

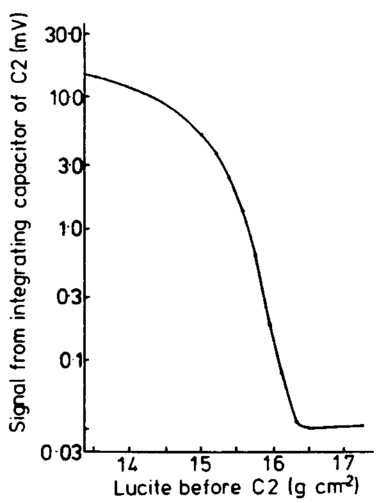

Fig. 2. Signal from C2 as a function of absorber thickness before it, for a given charge from C1.

a typical result which resembles a range curve for protons. The important point for proton tomography is the very rapid fall off of this curve. It is related to the very rapid fall off of the number–distance curve near the end of the range of monoenergetic protons passing through an absorber, but it is not strictly proportional to it. For our scintillation counters what is measured is the light output of those protons which penetrate the absorber and are stopped in the scintillator which is certainly able to accept the spread of the beam due to multiple scattering and probably has an unnecessarily large diameter for this purpose. The scintillators are also unnecessarily thick. Many different and probably better detector systems can be imagined. Each will have its own characteristically rapid fall off, and the reason in each case will be the rapid fall off of the number–distance curve mentioned above.

Another feature of fig. 2 is the flat region beyond the end of the range, the pedestal. This too will exist in all detector systems we can think of. In our case it is caused by the dark currents in the photomultipliers (about 25%) and the background of neutrons and γ-rays in the experimental area. We believe that the height of the pedestal can be reduced by a better choice of photomultipliers, scintillators and collimating system.

With a curve such as that shown in fig. 2 obtained for one counter the roles of the counters were interchanged and a similar curve was obtained for the other counter. From these curves a certain amount of absorber was chosen for each counter so as to put both at points on their response curves which had nearly the same high slope. The purpose of this procedure was to make the final measurements insensitive to small variations in the mean energy of the external proton beam. The amount of absorber before C1 was thereafter held constant. Measurements of the response of C2 were then made as a function of small variations about the amount of absorber before C2 chosen as described above.

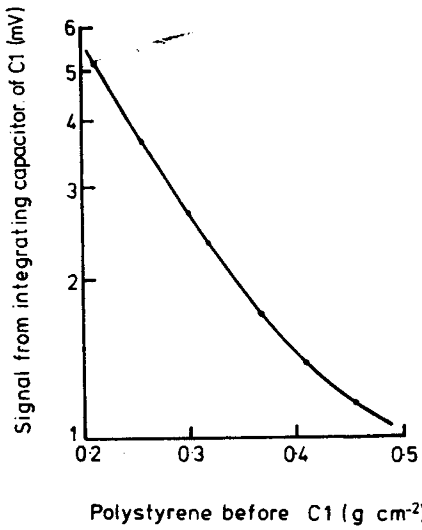

Fig. 3. Calibration curve of C2 with a fixed amount of absorber before C1.

The resulting calibration curve is shown in fig. 3, which demonstrates the power of the method. The curve is very roughly a straight line on a logarithmic plot. To simulate this curve with X-rays would require the use of X-rays with a mass absorption coefficient of about 6·6 $cm^2 g^{-1}$, and these would be attenuated by a factor of about $\exp(-84)$ in penetrating to a depth of 12·7 cm of Lucite, approximately the amount of absorber before each counter.

Having obtained this calibration curve we replaced the absorber before C2 by the phantom. This was an almost parallel-sided block of Lucite 12·70 cm wide and 5·08 cm thick with a circular hole and a concentric annular slot cut into it as shown in fig. 4. The radius of the hole was 1·59 cm, and the inner and outer radii of the annular region were 3·18 cm and 4·76 cm. The depths of both the hole and the slot were 4·76 cm. Provision was made for a peg of diameter 4·75 mm to be inserted at the centre of the hole. The phantom could be driven or scanned horizontally in a direction perpendicular to the incident proton beam which was defined by a slit in collimator D 2 mm wide horizontally and 8 mm high. The phantom was stepped across the proton beam in one or two millimetre steps in order to make a scan. The steps were chosen so that for one position of the phantom the proton beam coincided, within 0·2 mm, with the centre of the hole and slot. A scan was begun with the proton beam passing solely through Lucite and not intersecting the slot, and ended with the proton beam again passing solely through Lucite but on the other side of the hole and slot. The measurements made when the proton beam was a distance p from the centre of the hole were averaged with those made with the proton beam in the symmetrical position on the other side of the centre. This was done to compensate for the slight (0·5 milliradian) lack of parallelism of the sides of the phantom.

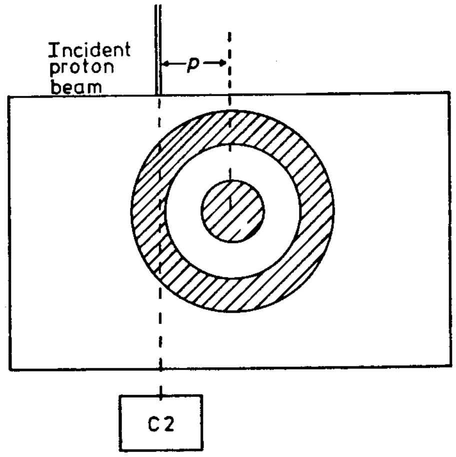

Fig. 4. The proton beam passes through the Lucite phantom and is detected by C2. Hatched areas represent a circular hole and a concentric annular slot containing sugar solution. The proton beam is p cm from the centre of the hole.

Four scans were made with both hole and annulus filled with a solution of sugar in water. In the first three scans the concentration of sugar was chosen to give a density of 1% less than the density of Lucite, and in the fourth the density was 0·5% less. Of the first three scans the first was made without any peg at the centre, the second was made with a polystyrene peg and the third was made with a Lucite peg. The measured values of the densities of the substances used are shown in table 1. There is a considerable uncertainty in the fourth decimal place hence we state our density differences as 0·012 and 0·006 g cm^{-3} for the two sugar solutions, and 0·135 g cm^{-3} for the polystyrene peg.

A number of measurements were made when the proton beam was passing through Lucite only on both sides of the annulus. At intermediate positions three observations were made. Each observation consisted of the measurement of the voltage on the integrating capacitor of C2 for a pre-set amount of charge from C1. The range of voltage readings for all scans except a small part of scan 2 was 2·3 mV. In the excepted part of scan 2 it was 4·2 mV, this large excursion being caused by the polystyrene peg. The standard deviation of a single measurement in a group of measurements made under identical conditions ranged from 0·05 mV to 0·09 mV. We believe that these variations are primarily due to vertical movements of the primary beam, but small variations in the dark currents of the phototubes (observed) and in their gains (surmised) may also contribute. The photomultiplier dark currents were measured from time to time, and all measurements were corrected for them.

Table 1. Densities of substances used

Substance		Density ($g\,cm^{-3}$)
Lucite		1·181†
Polystyrene		1·046†
1% Sugar solution		1·1694‡
		1·1692‡
		1·1676§
	Average	1·1687
0·5% Sugar solution		1·1751‡
		1·1742‡
		1·1743§
	Average	1·1745

† From weights and dimensions of samples
‡ Independent measures using hydrometer.
§ Calculated from density concentration tables.

The average of the measurements made when the proton beam was a distance p from the centre of the hole and the average of the measurements made when the beam passed through Lucite only were used to infer, from the calibration curve, a deviation in the number of $g\,cm^{-2}$ in the proton beam caused by the presence of the sugar solution. This deviation is denoted by $f(p)$. In a given scan the value of f varies from zero to some maximum, and the largest maximum encountered was 0·8 $g\,cm^{-2}$. The error in f is typically 0·005 $g\,cm^{-2}$.

4. Analysis

If $\rho(r)$ is the density at a distance r from the centre of a circularly symmetric density distribution (in our case ρ is the difference from the density of Lucite), and if $f(p)$ is the line integral of the density along a straight line which is a distance p from the centre, then

$$\rho(r) = \frac{d}{dr}\left(\frac{-r}{\pi}\int_r^{\infty}\frac{f(p)\,dp}{p(p^2-r^2)^{\frac{1}{2}}}\right) \equiv \frac{dJ(r)}{dr} \qquad (1)$$

This can be seen from eqn (26) of Cormack (1963) or, better, from first principles by writing down the integral expression for $f(p)$, noting that this is Abel's equation, the well known solution of which is eqn (1).

From the values of $f(p)$ found at a number of discrete values of p we calculated the values of $J(r)$ at values of r which are the same as the values of p by numerical integration of the integral in eqn (1). A linear interpolation between neighbouring values of $f(p)$ was used to evaluate the integral analytically from the singular point $p = r$ to the next value of p at which data had been taken. Simpson's rule was used to evaluate the rest of the integral. From these values of $J(r)$ its derivative, $\rho(r)$, was found by numerical differentiation.

5. Results

Running through the above analysis is the idea that density differences are all that matter for proton tomography. We shall continue this fiction a little longer for the presentation of the results. These are shown in figs 5 and 6, in

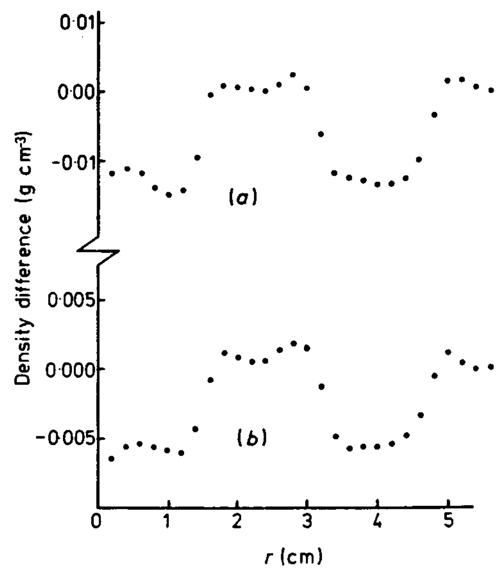

Fig. 5. Reconstructed radial distribution of density difference between Lucite and sugar solution, (*a*) with a density difference of 0·012 g cm^{-3}, (*b*) with a density difference of 0·006 g cm^{-3}. Note different scales on ordinates.

which density difference is plotted as a function of r. The results of the first and fourth scans are shown in fig. 5, those of the second and third scans are shown in fig. 6 but only for the region $r < 1$ cm. The principal feature of these results is that density differences of 0·5% and larger can be seen clearly and sharply using very rudimentary equipment. That the effective beam width near the centre of the phantom cannot be much more than the 2 mm entrance beam width can be seen most clearly in fig. 6. Any significant difference between the effects of the polystyrene and Lucite pegs has disappeared at $r = 5$ mm, while the sum of the radius of the peg and the entrance beam width is 4·4 mm. In addition to the smoothing introduced by the 2 mm beam width, an additional smoothing over a distance of 1–2 mm occurs as a result of the numerical differentiation of $J(r)$. There are two unexpected features of the reconstructions.

The first is the agreement of the reconstructed density differences with the measured values of 0·012 g cm^{-3} and 0·006 g cm^{-3} for the sugar solutions and 0·135 g cm^{-3} for the polystyrene peg. The second is the pattern of variation from the constancy of density difference which is expected in certain regions and the occurrence of this pattern in all scans including those parts of scans 2 and 3 which are not shown in fig. 6.

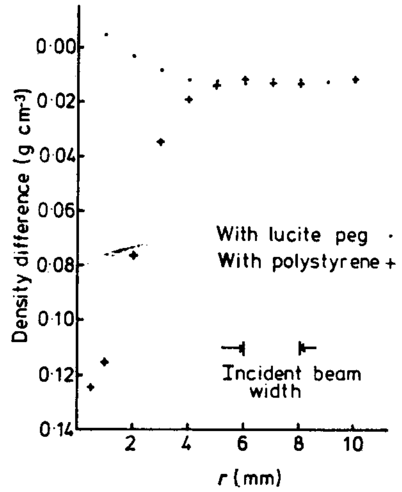

Fig. 6. Reconstructed radial distribution of density difference for the first 10 mm from the origin with Lucite and polystyrene pegs of diameter 4·75 mm centred at the origin. Density differences between Lucite and polystyrene and Lucite and sugar solution are 0·135 g cm^{-3} and 0·012 g cm^{-3} respectively.

The pertinent quantity in the slowing down of protons is not the density but the linear stopping power ratio. We have tried to calculate this for the sugar solutions using the results of Janni (1966) for protons. The problem is how to calculate, with the accuracy needed here, the stopping power of a compound knowing the stopping powers of either the elements it is made of or of similar compounds. We calculated the stopping power of the solutions by some interpolation method, then calculated the stopping power of Lucite by the same method and compared the latter with Janni's tabulated values for Lucite. In not one of the various methods tried was the difference less than 0·64%. The reason is not far to seek. Janni indicates that the agreement between calculated values and experimentally determined values is only at the 1% level. We have to conclude from our measurements that the relative stopping powers of the solutions and Lucite follow the densities quite accurately.

The variations of reconstructed density about constant values present a different problem. Some of them are artifacts introduced by the computer program, but one of them cannot be. This is the bump between 5·0 and 5·2 cm. The radius of the outer edge of the annulus is 4·763 cm so one would expect the density to be constant from 5·0 cm out even if the effective width of the beam was as high as 2·5 mm. However, this bump results from dips which occur consistently in all the raw data and which extend from 4·8 cm to 5·2 cm. We believe that this bump, and possibly parts of some of the others, are the result of a real physical effect caused by the sharp change in density and chemical composition at the outer edge of the annulus. It is possible that this is related to the effect discussed by West and Sherwood (1972, 1973) which depends on having a discontinuity in multiple scattering angle in a thin object being radiographed with protons. So far we have not been able to make a convincing case for this. However, the dips in the data are consistent with the pattern predicted by West and Sherwood if the multiple scattering in Lucite is greater than in the sugar solutions. This will be true if the change in density only determines the change in multiple scattering. As with the calculation of stopping power, neither the theory nor the available data enable us to calculate multiple scattering to the accuracy needed here. Whether or not the West–Sherwood effect is responsible for the dips in the data, they are there consistently and the only physical cause seems to be the discontinuity at the edge of the annulus. An effect of this sort might seriously affect the quality of a reconstruction if a large discontinuity were present in the sample, for example, the discontinuity between bone and surrounding soft tissue.

Since it is important for medical applications we mention that the entrance dose received by the phantom in order to determine $f(p)$ for a single value of p was 0·35 rad. This is high, but we made no effort to minimize the dose.

We would like to thank Dr. Giovanni Di Chiro and Dr. Rodney Brooks for encouraging us to do this experiment. We would also like to thank Robert A. Schmidt and Kristen Johnson for their assistance with the experiment.

Résumé

Tomographie quantitative des protons: expérimentations préliminaires

On a essayé de voir si l'on pouvait se servir de protons énergétiques (158 MeV) au lieu des rayons X dans la Tomographie Axiale à Ordination pour détecter les différences de densités de l'ordre de celles auxquelles les tomographes à rayons X du commerce cessent d'être utiles. Un fantôme circulairement symétrique se composant de solutions de sucre et de Lucite fut utilisé et des différences de densités de 0,5% furent reconstruites avec une assez bonne préçision à partir de données obtenues avec un équipement très simple. Des solutions de continuité dans soit la densité ou la composition chimique, ou bien les deux, semblent causer des artefacts dans la reconstruction. Ils peuvent être dûs à l'effet de West–Sherwood.

Zusammenfassung

Quantitative Protonentomographie: einleitende Experimente

Die Autoren untersuchen, ob Röntgenstrahlen in computerisierter Axial-Tomographie durch energetische Protonen (158 MeV) ersetzt werden können, um Dichteunterschiede in dem Bereich festzustellen, in dem kommerzielle Röntgentomographen nicht mehr von Nutzen sind. Verwendet wurde ein kreissymmetrisches Phantom aus Lutetium und Zuckerlösungen, und Dichteunterschiede von 0,5% wurden mit hinreichender Genauigkeit aufgrund von Daten rekonstruiert, die mit sehr einfachem Gerät aufgestellt worden waren. Diskontinuität in Dichte und/oder chemischer Zusammensetzung scheinen künstliche Erscheinungen in der Rekonstruktion zu verursachen. Dies mag mit dem West–Sherwood-Effekt in Verbindung stehen.

Резюме

Количественная томография с помощью протонов‘ предварительные эксперименты

Сделали попытку установить можно ли использовать энергетические протоны (158 МэВ) вместо рентгеновских лучей в томографии по оси с помощью ЭВМ для обнаружения разностей в плотности такого порядка, при которых коммерческие рентгеновские томографы неприменимы. Использовали периферийно симметрический фантом, содержащий растворы сахара и люсита и воспроизводились разности плотности 0,5% с относительно высокой точностью на основе данных, полученных с помощью очень простого оборудования. Отсутствие закономерностей в плотности или в химическом составе, или в обоих показателях кажется причиной артефактов в восстановлении. Эти артефакты возможно связаны с эффектом Веста–Шервуда.

References

Cormack, A. M., 1963, *J. Appl. Phys.*, **34**, 2722.

Cormack, A. M., 1964, *J. Appl. Phys.*, **35**, 2908.

Crow, K. M., Budinger, T. F., Cahoon, J. L., Elischer, V. P., Huesman, R. H., and Kanstein, L. L., 1975, *Lawrence Berkeley Laboratory Report* LBL–3812.

Janni, J. F., 1966, *U.S. Air Force Weapons Laboratory Report* AFWL–TR65–150.

Koehler, A. M., 1968, *Science, N.Y.*, **160**, 303.

Steward, V. W., and Koehler, A. M., 1973, *Nature, Lond.*, **245**, 38.

Steward, V. W., and Koehler, A. M., 1974, *Radiology*, **110**, 217.

West, D., and Sherwood, A. C., 1972, *Nature, Lond.*, **239**, 157.

West, D., and Sherwood, A. C., 1973, *Non-destructive Testing*, **6**, 249.